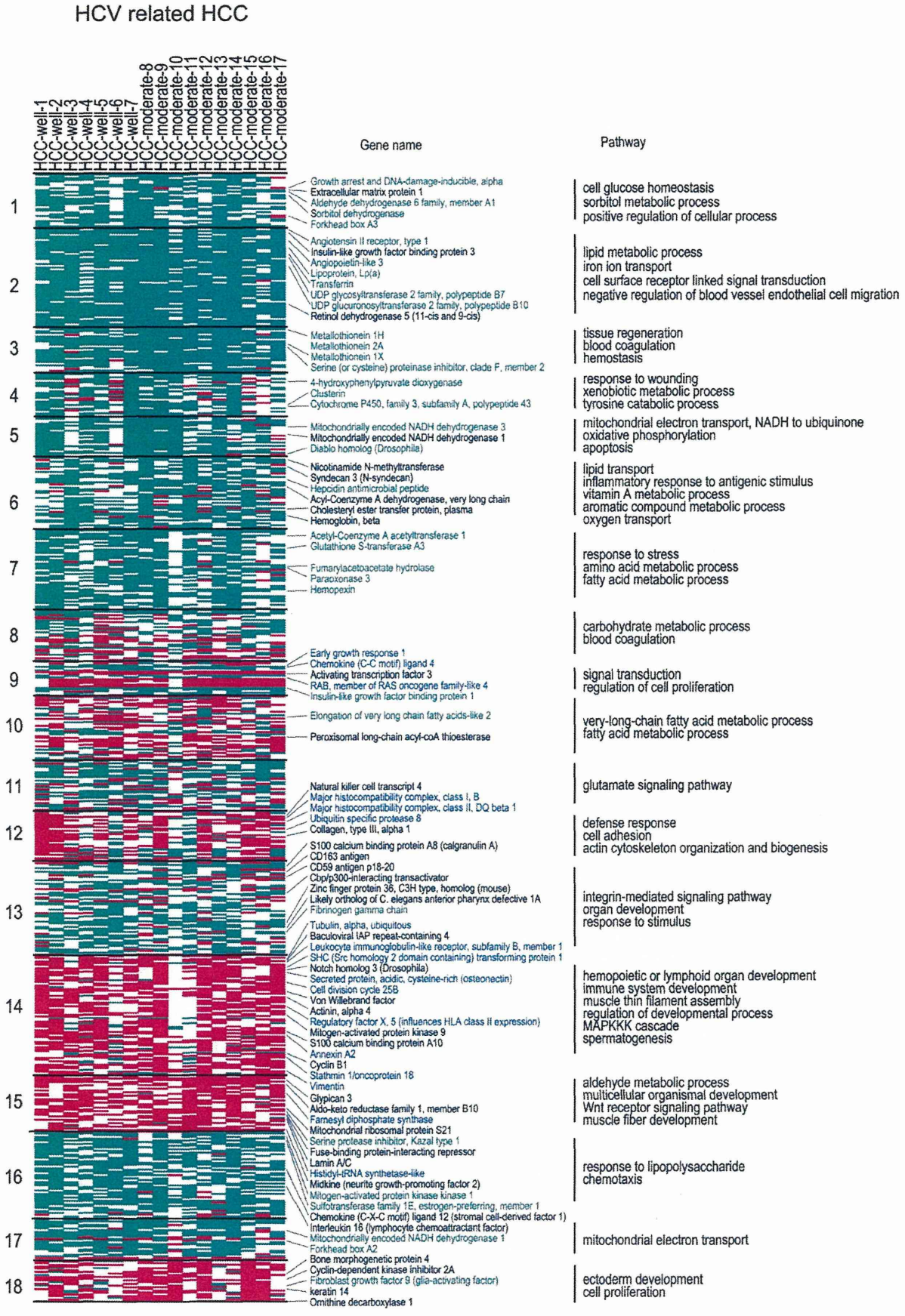
HCV related HCC
HCC-well-1
HCC-well-2
HCC-well-3
HCC-well-4
HCC-well-5
HCC-well-6
HCC-well-7
HCC-moderate-8
HCC-moderate-9
HCC-moderate-10
HCC-moderate-11
HCC-moderate-12
HCC-moderate-13
HCC-moderate-14
HCC-moderate-15
HCC-moderate-16
HCC-moderate-17
Gene name
Pathway
1
Growth arrest and DNA-damage-inducible, alpha
Extracellular matrix protein 1
Aldehyde dehydrogenase 6 family, member A1
Sorbitol dehydrogenase
Forkhead box A3
cell glucose homeostasis
sorbitol metabolic process
positive regulation of cellular process
2
Angiotensin II receptor, type 1
Insulin-like growth factor binding protein 3
Angiopoietin-like 3
Lipoprotein, Lp(a)
Transferrin
UDP glycosyltransferase 2 family, polypeptide B7
UDP glucuronosyltransferase 2 family, polypeptide B10
Retinol dehydrogenase 5 (11-cis and 9-cis)
lipid metabolic process
iron ion transport
cell surface receptor linked signal transduction
negative regulation of blood vessel endothelial cell migration
3
Metallothionein 1H
Metallothionein 2A
Metallothionein 1X
Serine (or cysteine) proteinase inhibitor, clade F, member 2
tissue regeneration
blood coagulation
hemostasis
4
4-hydroxyphenylpyruvate dioxygenase
Clusterin
Cytochrome P450, family 3, subfamily A, polypeptide 43
response to wounding
xenobiotic metabolic process
tyrosine catabolic process
5
Mitochondrially encoded NADH dehydrogenase 3
Mitochondrially encoded NADH dehydrogenase 1
Diablo homolog (Drosophila)
mitochondrial electron transport, NADH to ubiquinone
oxidative phosphorylation
apoptosis
6
Nicotinamide N-methyltransferase
Syndecan 3 (N-syndecan)
Hepcidin antimicrobial peptide
Acyl-Coenzyme A dehydrogenase, very long chain
Cholesteryl ester transfer protein, plasma
Hemoglobin, beta
lipid transport
inflammatory response to antigenic stimulus
vitamin A metabolic process
aromatic compound metabolic process
oxygen transport
7
Acetyl-Coenzyme A acetyltransferase 1
Glutathione S-transferase A3
Fumarylacetoacetate hydrolase
Paraoxonase 3
Hemopexin
response to stress
amino acid metabolic process
fatty acid metabolic process
8
carbohydrate metabolic process
blood coagulation
9
Early growth response 1
Chemokine (C-C motif) ligand 4
Activating transcription factor 3
RAB, member of RAS oncogene family-like 4
Insulin-like growth factor binding protein 1
signal transduction
regulation of cell proliferation
10
Elongation of very long chain fatty acids-like 2
Peroxisomal long-chain acyl-coA thioesterase
very-long-chain fatty acid metabolic process
fatty acid metabolic process
11
Natural killer cell transcript 4
Major histocompatibility complex, class I, B
Major histocompatibility complex, class II, DQ beta 1
glutamate signaling pathway
12
Ubiquitin specific protease 8
Collagen, type III, alpha 1
defense response
cell adhesion
13
S100 calcium binding protein A8 (calgranulin A)
CD163 antigen
CD59 antigen p18-20
Cbp/p300-interacting transactivator
Zinc finger protein 36, C3H type, homolog (mouse)
Likely ortholog of C. elegans anterior pharynx defective 1A
Fibrinogen gamma chain
Tubulin, alpha, ubiquitous
Baculoviral IAP repeat-containing 4
Leukocyte immunoglobulin-like receptor, subfamily B, member 1
SHC (Src homology 2 domain containing) transforming protein 1
actin cytoskeleton organization and biogenesis
integrin-mediated signaling pathway
organ development
response to stimulus
14
Notch homolog 3 (Drosophila)
Secreted protein, acidic, cysteine-rich (osteonectin)
Cell division cycle 25B
Von Willebrand factor
Actinin, alpha 4
Regulatory factor X, 5 (influences HLA class II expression)
Mitogen-activated protein kinase 9
S100 calcium binding protein A10
Annexin A2
Cyclin B1
hemopoietic or lymphoid organ development
immune system development
muscle thin filament assembly
regulation of developmental process
MAPKKK cascade
spermatogenesis
15
Stathmin 1/oncoprotein 18
Vimentin
Glypican 3
Aldo-keto reductase family 1, member B10
Farnesyl diphosphate synthase
Mitochondrial ribosomal protein S21
aldehyde metabolic process
multicellular organismal development
Wnt receptor signaling pathway
muscle fiber development
16
Serine protease inhibitor, Kazal type 1
Fuse-binding protein-interacting repressor
Lamin A/C
Histidyl-tRNA synthetase-like
Midkine (neurite growth-promoting factor 2)
Mitogen-activated protein kinase kinase 1
Sulfotransferase family 1E, estrogen-preferring, member 1
Chemokine (C-X-C motif) ligand 12 (stromal cell-derived factor 1)
Interleukin 16 (lymphocyte chemoattractant factor)
response to lipopolysaccharide
chemotaxis
17
Mitochondrially encoded NADH dehydrogenase 1
Forkhead box A2
mitochondrial electron transport
18
Bone morphogenetic protein 4
Cyclin-dependent kinase inhibitor 2A
Fibroblast growth factor 9 (glia-activating factor)
keratin 14
Ornithine decarboxylase 1
ectoderm development
cell proliferation

Table 2
Characteristic genes expressed in CH-C-related HCC.

Genes	Symbol	GenBank ID	Cluster No.	Up- or down-regulated	GO
Acetyl-coenzyme A acetyltransferase 1	ACAT1	NM_000019	7	Down	Metabolic process
Chemokine (C-C motif) ligand 19	CCL19	NM_006274	12	Up	Immune response
Natural killer cell transcript 4 (Interleukin 32)	IL32	NM_004221	12	Up	Immune response
Major histocompatibility complex, class I, B	HLA-B	NM_005514	12	Up	Immune response
Major histocompatibility complex, class II, DQ beta 1	HLA-DQB1	NM_002123	12	Up	Immune response
Ubiquitin specific protease 8	USP8	NM_005154	12	Up	Cell proliferation
Tubulin, alpha 1b	TUBA1B	NM_006082	14	Up	Microtubule cytoskeleton organization
Actin, alpha 2	ACTA2	NM_001613	14	Up	Vascular smooth muscle contraction
SHC transforming protein 1	SHC1	NM_183001	14	Up	Activation of MAPK activity
Sterile alpha motif domain containing 9	SAMD9	NM_017654	14	Up	Regulation of transcription, dna-dependent
S100 calcium binding protein A10	S100A10	NM_002964	14	Up	Signal transduction
Annexin A2	ANXA2	NM_017654	14	Up	Skeletal system development
Cyclin B1	CCNB1	M25753	14	Up	Cell cycle
Platelet-activating factor acetylhydrolase 1b, 3	PAFAH1B3	D63391	14	Up	Spermatogenesis
Vimentin	VIM	NM_003380	14	Up	Cell motion
Glypican 3	GPC3	NM_004484	15	Up	Anatomical structure morphogenesis
Aldo-keto reductase family 1, member B10	AKR1B10	NM_020299	15	Up	Cellular aldehyde metabolic process
ATP citrate lyase	ACLY	AI819617	15	Up	Lipid biosynthetic process
Farnesyl diphosphate synthase	FDPS	NM_002004	15	Up	Cholesterol biosynthetic process
Serine protease inhibitor, Kazal type 1	SPINK1	NM_003122	15	Up	Protein binding
Bone morphogenetic protein 4	BMP4	D30751	18	Up	Germ cell development
Cyclin-dependent kinase inhibitor 2A	CDKN2A	L27211	18	Up	Cell cycle checkpoint
Fibroblast growth factor 9	FGF9	D14838	18	Up	Signal transduction
Ornithine decarboxylase 1	ODC1	NM_002539	18	Up	Positive regulation of cell proliferation

Analysis of the individual gene interactions (Fig. 4B) showed that a key regulator gene of non-cancerous cluster No. 1, signal transducer and activator of transcription 1 (STAT1), negatively regulated early growth response protein 1 (EGR1) in HCC cluster No. 9 [24]. EGR1 was a key regulator of angiogenesis and fibrogenesis-inducing genes, such as PAI-1 (No. 9), COL1A1, and FAK1 (No. 18) [25–27]. In addition, EGR1 negatively regulated a key regulator of gluconeogenesis, PEPCK (No. 2) [28]. Thus, EGR1 regulated the tissue repair response as well as the metabolic process. In addition to STAT1, phosphatase and tensin homolog (PTEN), in non-cancerous cluster No. 7, negatively regulated FAK1 in HCC cluster No. 18 [29]. FAK1 regulated oncogene SHC (No. 14) and might be involved in the cancer signaling pathway [30,31]. Interestingly, PTEN was associated with Oct-3/4, a regulator of liver differentiation through its target gene C/EBP alpha (No. 3); C/EBP alpha regulated CYP27A1 and CYP3A5 (No. 5). Thus, in CH-C, two antitumor genes, STAT1 and PTEN, were associated with the expression of EGR1 and FAK1, which promote angiogenesis, fibrogenesis, and tumorigenesis in cancerous lesions. Interestingly, the expression of PTEN was related to the metabolic process of CH-C.

2.6. Serial gene expression in non-cancerous gene clusters and the occurrence of HCC

Analysis of the framework of gene clusters in relation to hepatocarcinogenesis by GGM and individual gene interactions revealed several key genes that were associated with hepatocarcinogenesis in non-cancerous clusters. We focused on STAT1 and PTEN in non-cancerous clusters in CH-C and evaluated serial changes of their expression at 2 time points (tumor free and tumor present) in additional 11 patients. The clinical characteristics of these patients at both time points are shown in Supplemental Table J. The expression of STAT1 and its related genes significantly decreased at the time of HCC development compared with the tumor-free time. Similarly, the expression of PTEN significantly decreased when HCC developed compared with the tumor-free time (Supplemental Fig. C2, 3).

3. Discussion

HCC frequently develops in the advanced stage of liver fibrosis. Although gene expression profiling of HCC and the background liver has been studied extensively [32–35], the relationship between the gene expression profiles of different lesions has not been elucidated. In the present study, we utilized GGM [15,16] to analyze the relationship between gene expression in HCC and non-cancerous liver. GGM is widely utilized to study gene association networks [12–14].

We first performed gene expression profiling in CH-B- and CH-C-related HCC. The up- and down-regulated genes were identified by a comparison with a single reference sample of normal liver. There may be some variations in gene expression among normal livers; however, the identified genes were characteristic of HCC and were consistent with previous reports [33,34]. Differences in the signaling pathways between CH-B- and CH-C-related HCC are clearly shown in Figs. 1 and 2 and Supplemental Fig. D. In CH-C-related HCC, immune response- and cytoskeleton-related genes, such as actin, tubulin, and vimentin, were up-regulated, while in CH-B-related HCC, cell matrix interaction genes, such as collagen IV and matrix metalloproteinase, were up-regulated. HBV-X protein reportedly promotes HCC metastasis by the up-regulation of matrix metalloproteinases [36]. The differences in the gene expression profiles between CH-C- and CH-B-related HCC were concordant with those reported previously [34,37].

In the present study, GGM analysis also revealed the interactions of each cluster within HCC as well as within non-cancerous lesions. GGM analysis in CH-B-related HCC showed that 3 up-regulated clusters and 6 down-regulated clusters were associated with each other. In CH-C-related HCC, 4 up-regulated gene clusters and 5 down-regulated gene clusters were associated with each other (Fig. 3). Interestingly, the up-regulated gene clusters were preferentially expressed in CPA in the liver. This prompted us to consider the origin of the HCC cells. Recent reports of immunohistochemical staining of liver tissue using stem cell markers, such as EpCAM and CD133, have suggested the presence of hepatic stem cells in the periportal area [38]. In contrast, many of the down-regulated genes were liver function and metabolism-related genes that were preferentially expressed in CLL in the liver.

Fig. 2. One way hierarchical clustering of 668 differentially expressed genes in CH-B-related HCC.A total of 668 genes were differentially expressed in CH-C-related HCC. Up-regulated genes are shown in red, down-regulated genes are shown in green, and unchanged genes are shown in white (Fig. 2).

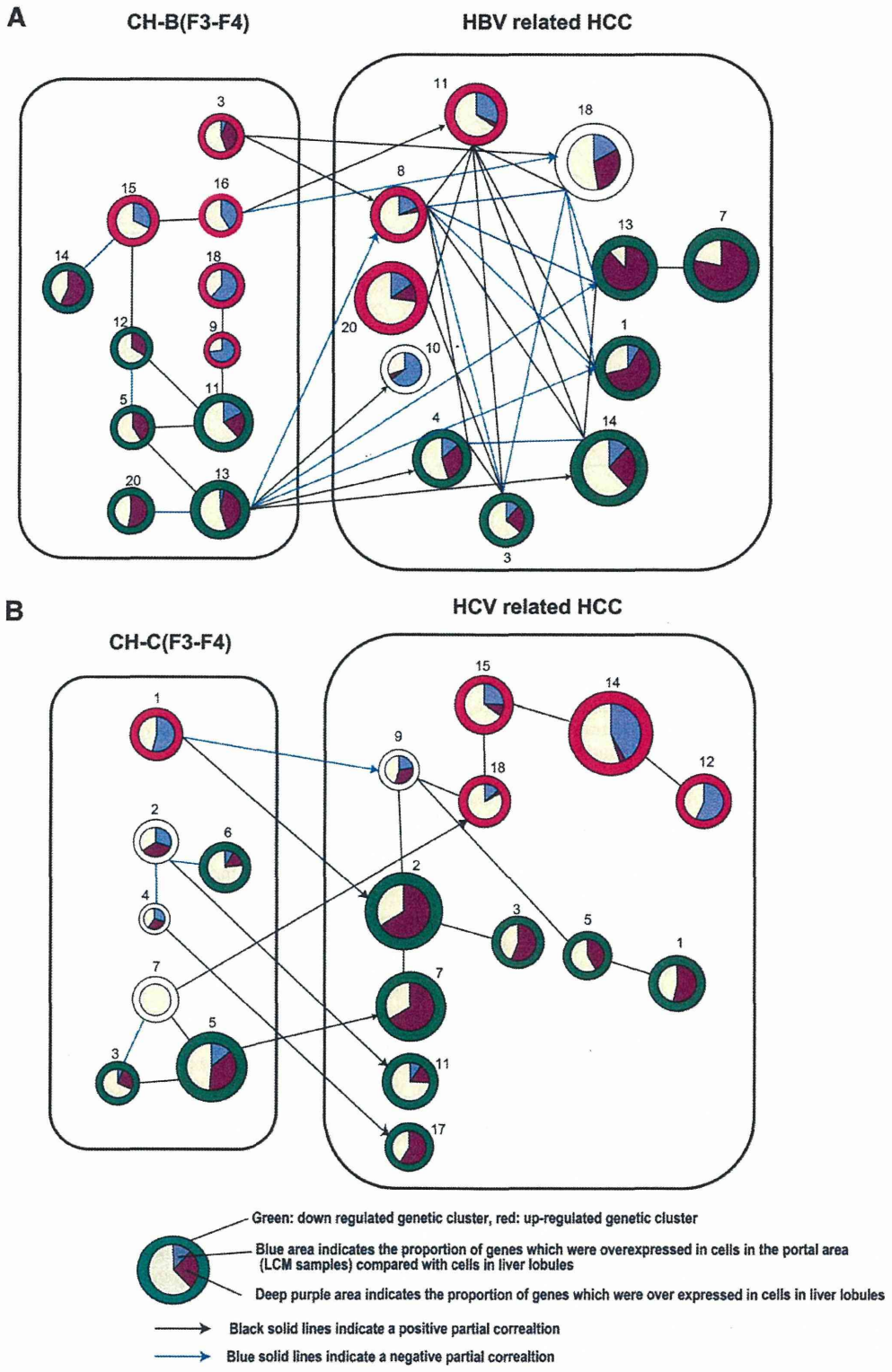

Fig. 3. GGM analysis of each cluster in HCC and non-cancerous lesions. Each cluster in the HCC and non-cancerous lesions was connected according to partial correlation coefficient matrix (PCCM) by GGM algorithms (Supplemental Tables H and I). The blue lines indicate a negative partial correlation and the black lines indicate a positive partial correlation. The size of each cluster reflects the number of clustered genes. The red circles are up-regulated gene clusters, while the green circles are down-regulated gene clusters. Within each cluster, the blue area indicates the proportion of genes that are over-expressed in CPA, while the deep purple area indicates the proportion of genes that are over-expressed in CLL. A; interactions of HBV related clusters. B; interactions of HCV related clusters.

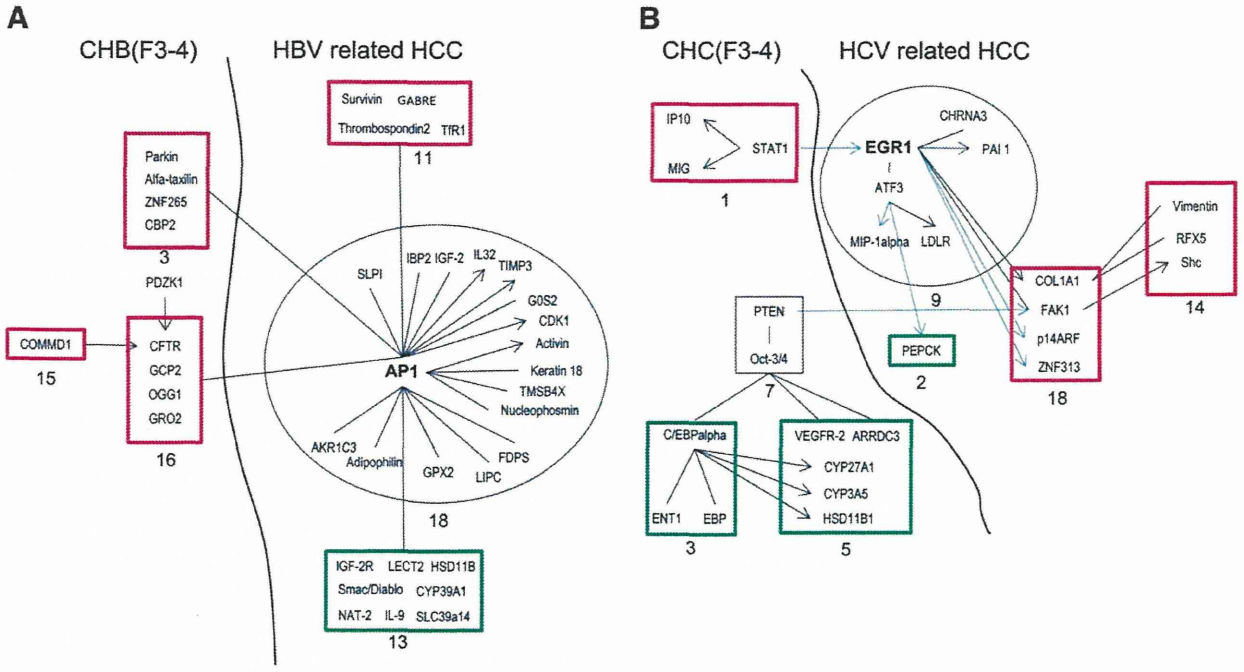

Fig. 4. Individual gene interactions between gene clusters in HCC and non-cancerous lesions. Direct interactions of individual genes among each cluster were confirmed by reference to the MetaCore database. The blue arrows indicate negative regulation, while the black arrows indicate positive regulation. Unspecified interactions are shown with black lines. The red squares are up-regulated gene clusters, while the green squares are down-regulated gene clusters. A; direct interactions of genes in HBV related clusters. B; direct interactions of genes in HCV related clusters.

GGM analysis between the HCC and non-cancerous liver revealed the unique interactions of 2 lesions in this study. In CH-B, up-regulated cluster Nos. 3 and 16, development and DNA damage response gene clusters, regulated HCC cluster Nos. 8, 11, and 18, VEGF-family signaling, apoptosis and survival-related, and ESR1 regulation of G1/S transition-related gene clusters. Down-regulated cluster No. 13, a metabolism-related gene cluster, negatively regulated the up-regulated HCC cluster No. 8. These results suggest that the metabolic status of non-cancerous liver influences the gene expression of HCC. Individual gene interactions with reference to the MetaCore database showed that 8 genes in non-cancerous cluster Nos. 3 and 16 were directly associated with AP1 in HCC cluster No. 18, which regulated the expression of many HCC genes (Fig. 4) [18–23]. Interestingly, the HBV transcript was clustered in HCC cluster No. 18. It has been reported that the HBV transcript enhances AP-1 activation [39,40]. The results suggest a role for the HBV transcript in CH-B-related HCC. Recently, a next generation sequencing approach revealed the frequent integration of HBV in HCC (86.4%), where the putative cancer-related human telomerase reverse transcriptase (hTERT), mixed-lineage leukemia 4, and cyclin E1 genes were located [41]. Although, we could not find the up-regulation of these genes in CH-B-related HCC, HBV genome integration should have important roles for HBV-related hepatocarcinogenesis. A previous report demonstrated that HBx retained the ability to overcome active oncogene RAS-induced senescence by using hTERT, which was introduced into human immortalized primary cells [42].

In CH-C, STAT1 and PTEN signaling in cluster Nos. 1 and 7, respectively, were associated with HCC cluster Nos. 9, 18, and 2, EGR1 signaling, ectodermal development and cell proliferation, lipid metabolism, and iron transport gene clusters. Individual gene interactions with reference to the MetaCore database showed that EGR1 regulates multiple genes in HCC cluster No. 9 as well as genes in up-regulated HCC cluster No. 18 and down-regulated HCC cluster No. 2 (Fig. 4). STAT1 and PTEN in non-cancerous cluster Nos. 1 and 7 exhibited an anti-tumor effect.

STAT1 negatively regulated EGR1 [24] and, interestingly, the expression of PTEN was associated with metabolic-related genes in non-cancerous cluster Nos. 3 and 5 (Fig. 4). PTEN reportedly promotes oxidative phosphorylation, decreases glycolysis, and prevents the metabolic reprogramming of cancer cells [43].

The reduced expression of these antitumor genes in CH-C might increase the expression of EGR1 and FAK1, which promote angiogenesis, fibrogenesis, and tumorigenesis in HCC (Fig. 4). EGR-1 promotes hepatocellular mitotic progression [44], while p53 and PTEN are downstream targets of EGR1. EGR1 might be involved in a negative feedback mechanism of cell cycle progression by inducing p53 and PTEN [45]. Recent reports described the tumorigenic role of EGR1 in the presence of p53 and PTEN mutations [46,47]. Thus, interferon signaling evoked by an innate immune response and the PTEN expression-associated metabolic process (Nos. 3 and 5) will likely regulate the gene expression profile of HCC through EGR1.

It is reported that HBV X protein represses the expression of PTEN by inhibiting the function of p53 [48] and c-Jun promotes cellular survival by suppression of PTEN [49]. In this study, the expression of PTEN was repressed in CH-B (Supplemental Fig. B, CH-B, cluster 21). Possible involvement of HBx, AP-1 and PTEN signaling in HBV-related hepatocarcinogenesis should be explored furthermore.

Recently, Hoshida et al. reported that gene expression profiling of the background liver of patients with HCC predicts their outcome [35]. In their report, gene sets, which correlated with good survival, included many metabolic process genes, such as those of fatty acid, amino acid, and glucose metabolism. In accordance with their results, our findings showed that the possible involvement of metabolic process genes in the background liver might influence gene expression in HCC. In addition, our study revealed the predisposing changes of gene expression in non-cancerous liver that precede the changes of gene expression in HCC. Interestingly, we found that the expression of the anti-tumor genes STAT1 and PTEN was decreased significantly at the onset of HCC compared with the tumor-free time. Therefore, serial analysis of the expression of these genes might be useful for predicting the development of HCC. Several reports have shown that the decreased expression of some chemokines, such as CXCL10, CCL2, and CCL5, is associated with the poor prognosis of resectable HCC [50,51]. In this study, the expression of CXCL10, CXCL6, CXCL9,

and macrophage migration inhibitory factor was decreased at the onset of HCC compared with the tumor-free time (Supplemental Fig. C). It would be worthwhile to examine the expression of these genes in serum samples to predict the development of HCC.

In summary, using a bioinformatics approach, we performed gene expression profiling of HCC and non-cancerous liver, which revealed the predisposing changes of gene expression in HCC. This approach will be useful for the early diagnosis of HCC. Further studies with a larger sample population are needed to confirm our data and to determine possible means for preventing the development of HCC.

4. Materials and methods

4.1. Patients and tissue samples

HCC and non-cancerous liver specimens were obtained from 17 patients with HCV-related HCC and 17 with HBV-related HCC who underwent surgical resection of the liver (Supplemental Tables A and B). For the control normal liver, a surgically obtained tissue sample from a patient who showed no clinical signs of hepatitis was used as described previously [9,10]. The liver tissue was histologically normal, and the patient tested negative for all hepatitis virus markers and had normal levels of serum aminotransferase. HCC and non-cancerous liver tissues were enucleated from resected specimens and frozen immediately in liquid nitrogen for RNA isolation [10]. In a previous study, expression profiling of the liver of 19 patients with CH-B and 18 with CH-C was performed (Table 2) [10]. The other experimental procedures are described in the Supplemental Materials and Methods.

4.2. Microarray analysis

cDNA microarray slides (Liver chip 10 k) were used as described previously [10]. For the selection of genes, we utilized data from the cDNA microarray and hepatic SAGE libraries derived from normal liver, CH-C, CH-C-related HCC, CH-B, and CH-B-related HCC, including 52,149 unique tags. We selected 9614 non-redundant genes that are expressed in diseased and normal liver. The detailed procedures for the preparation of the cDNA microarray slides are described in the Supplemental Material and Methods. RNA isolation, amplification of antisense RNA, labeling, and hybridization were performed according to the protocols described previously [10]. Quantitative assessment of the signals on the slides was performed by scanning on a ScanArray 5000 (General Scanning, Watertown, MA) followed by image analysis using GenePix Pro 4.1 (Axon Instruments, Union City, CA) as described previously [10]. The microarray data have been submitted to the Gene Expression Omnibus (GEO) public database at NCBI (Accession No. GSE41804). The details are also described in the Supplemental Material and Methods.

4.3. Graphical Gaussian modeling data processing

GGM [15,16] enabled us to reveal the gene cluster framework in relation to hepatocellular carcinogenesis of CH-B and CH-C. The procedure included: 1) gene clustering; 2) construction of the PCCM by GGM algorithms; and 3) visualization of the cluster pathway (Supplemental Fig. A).

4.4. Gene selection

To utilize a variety of tissue samples, we first calculated the ratio of gene expression in non-cancerous tissue (36 with CH-B and 35 with CH-C) to that in normal tissue and the ratio of gene expression in HCC tissue (17 with CH-B related HCC and 17 with CH-C related HCC) to that in normal tissue. Then, the expression ratios of non-cancerous and HCC tissues in individual samples were standardized in the two tissues, respectively, by transformation to the Z score (each value was subtracted by the average value and divided by the standard deviation (SD)) such that the mean expression value was 0 and the SD was 1. A gene was regarded as differentially expressed if the Z score was >1 or <-1 ($1 > |AV \pm SD|$). Although the criterion for a differentially expressed gene is usually $|AV \pm 2SD|$, the selection procedure described above is simply designed to gather as many differentially expressed genes as possible, and is suitable for determining the macroscopic relationships between gene systems estimated by cluster analysis. Gene selection from non-HCC samples was performed similarly by avoiding the selected genes in HCC (backward selection). Therefore, a correlation between HCC and non-HCC genes could be obtained as there was no overlap between the genes.

4.5. Clustering with automatic determination of cluster number

In gene profile clustering, the Euclidian distance between Pearson's correlation coefficient of profiles and the unweighted pair group method using the arithmetic average (UPGMA or group average method) were adopted as the metric and the technique, respectively, with reference to previous GGM analysis [15,16]. Note that the present metric and technique were selected to estimate robustly the clusters against the noise of gene expression measurements [15]. In cluster number estimation, the variance inflation factor was adopted as a stopping rule for the hierarchical clustering of expression profiles [15], and the popular cutoff value of 10.0 [52] was adopted as the threshold.

4.6. Graphical Gaussian modeling

The average expression profiles were calculated for the members of each cluster, and the average correlation coefficient matrix between the clusters was calculated. The average correlation coefficient matrix between the clusters was then subjected to GGM as described previously [15,16]. The correlation coefficient can return a false value in the presence of confounding factors. Partial correlation enables replacement of a false-positive correlation with the actual correlation. The PCCM was calculated using GGM (Supplemental Fig. A). All calculations for clustering analysis and GGM were performed via the ASIAN web site (http://eureka.cbrc.jp/asian/index_j.html) [53] and "Auto Net Finder," a commercial desktop version of ASIAN (Infocom Corporation, Shibuya, Tokyo, Japan, http://www.infocom.co.jp/bio/download/).

4.7. Rearrangement of the inferred network

Since the magnitude of the partial correlation coefficient indicates the strength of the association between clusters, the intact network can be rearranged according to the partial correlation coefficient to interpret the association between clusters. The strength of the association can be assigned by a standard test for the partial correlation coefficient. In the present study, the significance level in the t-test was 1% (Supplemental Fig. A).

4.8. Gene ontology of cluster members

Functional ontology enrichment analysis was performed to examine the gene ontology process distribution of each cluster gene using MetaCore™ (Thomson Reuters, New York, NY). Gene ontology was also confirmed by DAVID Bioinformatics Resources 6.7 (http://david.abcc.ncifcrf.gov/) [17].

Supplementary data to this article can be found online at http://dx.doi.org/10.1016/j.ygeno.2013.02.007.

Acknowledgments

The authors thank Nami Nishiyama for excellent technical assistance.

References

[1] R. Siegel, D. Naishadham, A. Jemal, Cancer statistics, 2012, CA Cancer J. Clin. 62 (2012) 10–29.
[2] H. Tsukuma, T. Hiyama, S. Tanaka, M. Nakao, T. Yabuuchi, T. Kitamura, K. Nakanishi, I. Fujimoto, A. Inoue, H. Yamazaki, Risk factors for hepatocellular carcinoma among patients with chronic liver disease, N. Engl. J. Med. 328 (1993) 1797–1801.
[3] A. Arzumanyan, H.M. Reis, M.A. Feitelson, Pathogenic mechanisms in HBV- and HCV-associated hepatocellular carcinoma, Nat. Rev. Cancer 13 (2012) 123–135.
[4] H. Yoshida, Y. Shiratori, M. Moriyama, Y. Arakawa, T. Ide, M. Sata, O. Inoue, M. Yano, M. Tanaka, S. Fujiyama, S. Nishiguchi, T. Kuroki, F. Imazeki, O. Yokosuka, S. Kinoyama, G. Yamada, M. Omata, Interferon therapy reduces the risk for hepatocellular carcinoma: national surveillance program of cirrhotic and noncirrhotic patients with chronic hepatitis C in Japan. IHIT Study Group. Inhibition of hepatocarcinogenesis by interferon therapy, Ann. Intern. Med. 131 (1999) 174–181.
[5] G. Fattovich, T. Stroffolini, I. Zagni, F. Donato, Hepatocellular carcinoma in cirrhosis: incidence and risk factors, Gastroenterology 127 (2004) S35–S50.
[6] A. de La Coste, B. Romagnolo, P. Billuart, C.A. Renard, M.A. Buendia, O. Soubrane, M. Fabre, J. Chelly, C. Beldjord, A. Kahn, C. Perret, Somatic mutations of the beta-catenin gene are frequent in mouse and human hepatocellular carcinomas, Proc. Natl. Acad. Sci. U. S. A. 95 (1998) 8847–8851.
[7] D.F. Calvisi, S. Ladu, A. Gorden, M. Farina, E.A. Conner, J.S. Lee, V.M. Factor, S.S. Thorgeirsson, Ubiquitous activation of Ras and Jak/Stat pathways in human HCC, Gastroenterology 130 (2006) 1117–1128.
[8] G.H. Thoresen, T.K. Guren, D. Sandnes, M. Peak, L. Agius, T. Christoffersen, Response to transforming growth factor alpha (TGFalpha) and epidermal growth factor (EGF) in hepatocytes: lower EGF receptor affinity of TGFalpha is associated with more sustained activation of p42/p44 mitogen-activated protein kinase and greater efficacy in stimulation of DNA synthesis, J. Cell. Physiol. 175 (1998) 10–18.
[9] M. Honda, S. Kaneko, H. Kawai, Y. Shirota, K. Kobayashi, Differential gene expression between chronic hepatitis B and C hepatic lesion, Gastroenterology 120 (2001) 955–966.
[10] M. Honda, T. Yamashita, T. Ueda, H. Takatori, R. Nishino, S. Kaneko, Different signaling pathways in the livers of patients with chronic hepatitis B or chronic hepatitis C, Hepatology 44 (2006) 1122–1138.
[11] M. Honda, M. Nakamura, M. Tateno, A. Sakai, T. Shimakami, T. Shirasaki, T. Yamashita, K. Arai, T. Yamashita, Y. Sakai, S. Kaneko, Differential interferon signaling in liver lobule and portal area cells under treatment for chronic hepatitis C, J. Hepatol. 53 (2010) 817–826.
[12] H. Kishino, P.J. Waddell, Correspondence analysis of genes and tissue types and finding genetic links from microarray data, Genome Inform. Ser. Workshop Genome Inform. 11 (2000) 83–95.
[13] P.J. Waddell, H. Kishino, Cluster inference methods and graphical models evaluated on NCI60 microarray gene expression data, Genome Inform. Ser. Workshop Genome Inform. 11 (2000) 129–140.
[14] J. Krumsiek, K. Suhre, T. Illig, J. Adamski, F.J. Theis, Gaussian graphical modeling reconstructs pathway reactions from high-throughput metabolomics data, BMC Syst. Biol. 5 (2011) 21.
[15] H. Toh, K. Horimoto, Inference of a genetic network by a combined approach of cluster analysis and graphical Gaussian modeling, Bioinformatics 18 (2002) 287–297.
[16] S. Aburatani, F. Sun, S. Saito, M. Honda, S. Kaneko, K. Horimoto, Gene systems network inferred from expression profiles in hepatocellular carcinogenesis by graphical Gaussian model, EURASIP J. Bioinform. Syst. Biol. (2007) 47214.
[17] W. Huang da, B.T. Sherman, Q. Tan, J. Kir, D. Liu, D. Bryant, Y. Guo, R. Stephens, M.W. Baseler, H.C. Lane, R.A. Lempicki, DAVID bioinformatics resources: expanded annotation database and novel algorithms to better extract biology from large gene lists, Nucleic Acids Res. 35 (2007) W169–W175.
[18] L. Russell, D.R. Forsdyke, A human putative lymphocyte G0/G1 switch gene containing a CpG-rich island encodes a small basic protein with the potential to be phosphorylated, DNA Cell Biol. 10 (1991) 581–591.
[19] L. Zhong, J. Ou, U. Barkai, J.F. Mao, J. Frasor, G. Gibori, Molecular cloning and characterization of the rat ovarian 20 alpha-hydroxysteroid dehydrogenase gene, Biochem. Biophys. Res. Commun. 249 (1998) 797–803.
[20] K.M. Mani, C. Lefebvre, K. Wang, W.K. Lim, K. Basso, R. Dalla-Favera, A. Califano, A systems biology approach to prediction of oncogenes and molecular perturbation targets in B-cell lymphomas, Mol. Syst. Biol. 4 (2008) 169.
[21] H.K. Kwon, J.S. Hwang, J.S. So, C.G. Lee, A. Sahoo, J.H. Ryu, W.K. Jeon, B.S. Ko, C.R. Im, S.H. Lee, Z.Y. Park, S.H. Im, Cinnamon extract induces tumor cell death through inhibition of NFkappaB and AP1, BMC Cancer 10 (2010) 392.
[22] K.R. Mitchell, D. Warshawsky, Xenobiotic inducible regions of the human arylamine N-acetyltransferase 1 and 2 genes, Toxicol. Lett. 139 (2003) 11–23.
[23] D. Bottomly, S.L. Kyler, S.K. McWeeney, G.S. Yochum, Identification of {beta}-catenin binding regions in colon cancer cells using ChIP-Seq, Nucleic Acids Res. 38 (2010) 5735–5745.
[24] J.L. Ingram, A. Antao-Menezes, J.B. Mangum, O. Lyght, P.J. Lee, J.A. Elias, J.C. Bonner, Opposing actions of Stat1 and Stat6 on IL-13-induced up-regulation of early growth response-1 and platelet-derived growth factor ligands in pulmonary fibroblasts, J. Immunol. 177 (2006) 4141–4148.
[25] H. Liao, M.C. Hyman, D.A. Lawrence, D.J. Pinsky, Molecular regulation of the PAI-1 gene by hypoxia: contributions of Egr-1, HIF-1alpha, and C/EBPalpha, FASEB J. 21 (2007) 935–949.
[26] V. Lejard, F. Blais, M.J. Guerquin, A. Bonnet, M.A. Bonnin, E. Havis, M. Malbouyres, C.B. Bidaud, G. Maro, P. Gilardi-Hebenstreit, J. Rossert, F. Ruggiero, D. Duprez, EGR1 and EGR2 involvement in vertebrate tendon differentiation, J. Biol. Chem. 286 (2011) 5855–5867.
[27] V. Golubovskaya, A. Kaur, W. Cance, Cloning and characterization of the promoter region of human focal adhesion kinase gene: nuclear factor kappa B and p53 binding sites, Biochim. Biophys. Acta 1678 (2004) 111–125.
[28] S.P. Berasi, C. Huard, D. Li, H.H. Shih, Y. Sun, W. Zhong, J.E. Paulsen, E.L. Brown, R.E. Gimeno, R.V. Martinez, Inhibition of gluconeogenesis through transcriptional activation of EGR1 and DUSP4 by AMP-activated kinase, J. Biol. Chem. 281 (2006) 27167–27177.
[29] J. Gu, M. Tamura, R. Pankov, E.H. Danen, T. Takino, K. Matsumoto, K.M. Yamada, Shc and FAK differentially regulate cell motility and directionality modulated by PTEN, J. Cell Biol. 146 (1999) 389–403.
[30] J.F. Rual, K. Venkatesan, T. Hao, T. Hirozane-Kishikawa, A. Dricot, N. Li, G.F. Berriz, F.D. Gibbons, M. Dreze, N. Ayivi-Guedehoussou, N. Klitgord, C. Simon, M. Boxem, S. Milstein, J. Rosenberg, D.S. Goldberg, L.V. Zhang, S.L. Wong, G. Franklin, S. Li, J.S. Albala, J. Lim, C. Fraughton, E. Llamosas, S. Cevik, C. Bex, P. Lamesch, R.S. Sikorski, J. Vandenhaute, H.Y. Zoghbi, A. Smolyar, S. Bosak, R. Sequerra, L. Doucette-Stamm, M.E. Cusick, D.E. Hill, F.P. Roth, M. Vidal, Towards a proteome-scale map of the human protein–protein interaction network, Nature 437 (2005) 1173–1178.
[31] T.P. Hecker, J.R. Grammer, G.Y. Gillespie, J. Stewart, C.L. Gladson, Focal adhesion kinase enhances signaling through the Shc/extracellular signal-regulated kinase pathway in anaplastic astrocytoma tumor biopsy samples, Cancer Res. 62 (2002) 2699–2707.
[32] H. Okabe, S. Satoh, T. Kato, O. Kitahara, R. Yanagawa, Y. Yamaoka, T. Tsunoda, Y. Furukawa, Y. Nakamura, Genome-wide analysis of gene expression in human hepatocellular carcinomas using cDNA microarray: identification of genes involved in viral carcinogenesis and tumor progression, Cancer Res. 61 (2001) 2129–2137.
[33] Y. Hippo, K. Watanabe, A. Watanabe, Y. Midorikawa, S. Yamamoto, S. Ihara, S. Tokita, H. Iwanari, Y. Ito, K. Nakano, J. Nezu, H. Tsunoda, T. Yoshino, I. Ohizumi, M. Tsuchiya, S. Ohnishi, M. Makuuchi, T. Hamakubo, T. Kodama, H. Aburatani, Identification of soluble NH2-terminal fragment of glypican-3 as a serological marker for early-stage hepatocellular carcinoma, Cancer Res. 64 (2004) 2418–2423.
[34] Y. Shirota, S. Kaneko, M. Honda, H.F. Kawai, K. Kobayashi, Identification of differentially expressed genes in hepatocellular carcinoma with cDNA microarrays, Hepatology 33 (2001) 832–840.
[35] Y. Hoshida, A. Villanueva, M. Kobayashi, J. Peix, D.Y. Chiang, A. Camargo, S. Gupta, J. Moore, M.J. Wrobel, J. Lerner, M. Reich, J.A. Chan, J.N. Glickman, K. Ikeda, M. Hashimoto, G. Watanabe, M.G. Daidone, S. Roayaie, M. Schwartz, S. Thung, H.B. Salvesen, S. Gabriel, V. Mazzaferro, J. Bruix, S.L. Friedman, H. Kumada, J.M. Llovet, T.R. Golub, Gene expression in fixed tissues and outcome in hepatocellular carcinoma, N. Engl. J. Med. 359 (2008) 1995–2004.
[36] L. Xia, W. Huang, D. Tian, H. Zhu, Y. Zhang, H. Hu, D. Fan, Y. Nie, K. Wu, Upregulated FoxM1 expression induced by hepatitis B virus X protein promotes tumor metastasis and indicates poor prognosis in hepatitis B virus-related hepatocellular carcinoma, J. Hepatol. 57 (2012) 600–612.
[37] S. Ura, M. Honda, T. Yamashita, T. Ueda, H. Takatori, R. Nishino, H. Sunakozaka, Y. Sakai, K. Horimoto, S. Kaneko, Differential microRNA expression between hepatitis B and hepatitis C leading disease progression to hepatocellular carcinoma, Hepatology 49 (2009) 1098–1112.
[38] R. Turner, O. Lozoya, Y. Wang, V. Cardinale, E. Gaudio, G. Alpini, G. Mendel, E. Wauthier, C. Barbier, D. Alvaro, L.M. Reid, Human hepatic stem cell and maturational liver lineage biology, Hepatology 53 (2011) 1035–1045.
[39] K.M. Sze, G.K. Chu, J.M. Lee, I.O. Ng, C-terminal truncated HBx is associated with metastasis and enhances invasiveness via C-Jun / MMP10 activation in hepatocellular carcinoma, Hepatology (2012).
[40] Y. Tanaka, F. Kanai, T. Ichimura, K. Tateishi, Y. Asaoka, B. Guleng, A. Jazag, M. Ohta, J. Imamura, T. Ikenoue, H. Ijichi, T. Kawabe, T. Isobe, M. Omata, The hepatitis B virus X protein enhances AP-1 activation through interaction with Jab1, Oncogene 25 (2006) 633–642.
[41] W.K. Sung, H. Zheng, S. Li, R. Chen, X. Liu, Y. Li, N.P. Lee, W.H. Lee, P.N. Ariyaratne, C. Tennakoon, F.H. Mulawadi, K.F. Wong, A.M. Liu, R.T. Poon, S.T. Fan, K.L. Chan, Z. Gong, Y. Hu, Z. Lin, G. Wang, Q. Zhang, T.D. Barber, W.C. Chou, A. Aggarwal, K. Hao, W. Zhou, C. Zhang, J. Hardwick, C. Buser, J. Xu, Z. Kan, H. Dai, M. Mao, C. Reinhard, J. Wang, J.M. Luk, Genome-wide survey of recurrent HBV integration in hepatocellular carcinoma, Nat. Genet. 44 (2012) 765–769.
[42] N. Oishi, K. Shilagardi, Y. Nakamoto, M. Honda, S. Kaneko, S. Murakami, Hepatitis B virus X protein overcomes oncogenic RAS-induced senescence in human immortalized cells, Cancer Sci. 98 (2007) 1540–1548.
[43] A. Ortega-Molina, M. Serrano, PTEN in cancer, metabolism, and aging, Trends Endocrinol. Metab. (2012).
[44] Y. Liao, O.N. Shikapwashya, E. Shteyer, B.K. Dieckgraefe, P.W. Hruz, D.A. Rudnick, Delayed hepatocellular mitotic progression and impaired liver regeneration in early growth response-1-deficient mice, J. Biol. Chem. 279 (2004) 43107–43116.
[45] Y. Zwang, A. Sas-Chen, Y. Drier, T. Shay, R. Avraham, M. Lauriola, E. Shema, E. Lidor-Nili, J. Jacob-Hirsch, N. Amariglio, Y. Lu, G.B. Mills, G. Rechavi, M. Oren, E. Domany, Y. Yarden, Two phases of mitogenic signaling unveil roles for p53 and EGR1 in elimination of inconsistent growth signals, Mol. Cell 42 (2011) 524–535.
[46] J. Yu, S.S. Zhang, K. Saito, S. Williams, Y. Arimura, Y. Ma, Y. Ke, V. Baron, D. Mercola, G.S. Feng, E. Adamson, T. Mustelin, PTEN regulation by Akt-EGR1-ARF-PTEN axis, EMBO J. 28 (2009) 21–33.
[47] D. Lu, C. Han, T. Wu, Microsomal prostaglandin E synthase-1 promotes hepatocarcinogenesis through activation of a novel EGR1/beta-catenin signaling axis, Oncogene 31 (2012) 842–857.
[48] T.W. Chung, Y.C. Lee, J.H. Ko, C.H. Kim, Hepatitis B Virus X protein modulates the expression of PTEN by inhibiting the function of p53, a transcriptional activator in liver cells, Cancer Res. 63 (2003) 3453–3458.
[49] K. Hettinger, F. Vikhanskaya, M.K. Poh, M.K. Lee, I. de Belle, J.T. Zhang, S.A. Reddy, K. Sabapathy, c-Jun promotes cellular survival by suppression of PTEN, Cell Death Differ. 14 (2007) 218–229.

[50] V. Chew, C. Tow, M. Teo, H.L. Wong, J. Chan, A. Gehring, M. Loh, A. Bolze, R. Quek, V.K. Lee, K.H. Lee, J.P. Abastado, H.C. Toh, A. Nardin, Inflammatory tumour microenvironment is associated with superior survival in hepatocellular carcinoma patients, J. Hepatol. 52 (2010) 370–379.
[51] V. Chew, J. Chen, D. Lee, E. Loh, J. Lee, K.H. Lim, A. Weber, K. Slankamenac, R.T. Poon, H. Yang, L.L. Ooi, H.C. Toh, M. Heikenwalder, I.O. Ng, A. Nardin, J.P. Abastado, Chemokine-driven lymphocyte infiltration: an early intratumoural event determining long-term survival in resectable hepatocellular carcinoma, Gut 61 (2012) 427–438.
[52] R.J. Freund, W.J. Wilson, Regression analysis : statistical modeling of a response variable, Academic Press, San Diego, 1998.
[53] S. Aburatani, K. Goto, S. Saito, H. Toh, K. Horimoto, ASIAN: a web server for inferring a regulatory network framework from gene expression profiles, Nucleic Acids Res. 33 (2005) W659–W664.

HEPATOLOGY
Official Journal of the American Association for the Study of Liver Diseases

Discrete Nature of EpCAM$^+$ and CD90$^+$ Cancer Stem Cells in Human Hepatocellular Carcinoma

Taro Yamashita,[1] Masao Honda,[1] Yasunari Nakamoto,[1] Masayo Baba,[1] Kouki Nio,[1] Yasumasa Hara,[1] Sha Sha Zeng,[1] Takehiro Hayashi,[1] Mitsumasa Kondo,[1] Hajime Takatori,[1] Tatsuya Yamashita,[1] Eishiro Mizukoshi,[1] Hiroko Ikeda,[1] Yoh Zen,[1] Hiroyuki Takamura,[1] Xin Wei Wang,[2] and Shuichi Kaneko[1]

Recent evidence suggests that hepatocellular carcinoma (HCC) is organized by a subset of cells with stem cell features (cancer stem cells; CSCs). CSCs are considered a pivotal target for the eradication of cancer, and liver CSCs have been identified by the use of various stem cell markers. However, little information is known about the expression patterns and characteristics of marker-positive CSCs, hampering the development of personalized CSC-targeted therapy. Here, we show that CSC markers EpCAM and CD90 are independently expressed in liver cancer. In primary HCC, EpCAM$^+$ and CD90$^+$ cells resided distinctively, and gene-expression analysis of sorted cells suggested that EpCAM$^+$ cells had features of epithelial cells, whereas CD90$^+$ cells had those of vascular endothelial cells. Clinicopathological analysis indicated that the presence of EpCAM$^+$ cells was associated with poorly differentiated morphology and high serum alpha-fetoprotein (AFP), whereas the presence of CD90$^+$ cells was associated with a high incidence of distant organ metastasis. Serial xenotransplantation of EpCAM$^+$/CD90$^+$ cells from primary HCCs in immunedeficient mice revealed rapid growth of EpCAM$^+$ cells in the subcutaneous lesion and a highly metastatic capacity of CD90$^+$ cells in the lung. In cell lines, CD90$^+$ cells showed abundant expression of c-Kit and *in vitro* chemosensitivity to imatinib mesylate. Furthermore, CD90$^+$ cells enhanced the motility of EpCAM$^+$ cells when cocultured *in vitro* through the activation of transforming growth factor beta (TGF-β) signaling, whereas imatinib mesylate suppressed *TGFB1* expression in CD90$^+$ cells as well as CD90$^+$ cell-induced motility of EpCAM$^+$ cells. *Conclusion*: Our data suggest the discrete nature and potential interaction of EpCAM$^+$ and CD90$^+$ CSCs with specific gene-expression patterns and chemosensitivity to molecular targeted therapy. The presence of distinct CSCs may determine the clinical outcome of HCC. (HEPATOLOGY 2013;57:1484-1497)

The cancer stem cell (CSC) hypothesis, which suggests that a subset of cells bearing stem-cell–like features is indispensable for tumor development, has recently been put forward subsequent to advances in molecular and stem cell biology. Liver cancer, including hepatocellular carcinoma (HCC), is a leading cause of cancer death worldwide.[1] Recent studies have shown the existence of CSCs in liver cancer cell lines and primary HCC specimens using various stem cell markers.[2-7] Independently, we have identified novel HCC subtypes defined by the hepatic stem/progenitor cell markers,

Abbreviations: 5-FU, fluorouracil; Abs, antibodies; AFP, alpha-fetoprotein; CK-19, cytokeratin-19; CSC, cancer stem cell; DNs, dysplastic nodules; EMT, epithelial mesenchymal transition; EpCAM; epithelial cell adhesion molecule; FACS, fluorescent-activated cell sorting; HBV, hepatitis B virus; HCC, hepatocellular carcinoma; HCV, hepatitis C virus; HSCs, hepatic stem cells; IF, immunofluorescence; IHC, immunohistochemistry; IR, immunoreactivity; MDS, multidimensional scaling; NBNC, non-B, non-C hepatitis; NOD/SCID, nonobese diabetic, severe combined immunodeficient; NT, nontumor; OV-1, ovalbumin 1; qPCR, quantitative real-time polymerase chain reaction; SC, subcutaneous; Smad3, Mothers against decapentaplegic homolog 3; TECs, tumor epithelial cells; TGF-β, transforming growth factor beta; T/N, tumor/nontumor; VECs, vascular endothelial cells; VM, vasculogenic mimicry; VEGFR, vascular endothelial growth factor receptor.

From the [1]Liver Center, Kanazawa University Hospital, Kanazawa, Ishikawa, Japan; and [2]Laboratory of Human Carcinogenesis, Center for Cancer Research, National Cancer Institute, Bethesda, MD.

Received July 9, 2012; revised October 22, 2012; accepted November 6, 2012.

This study was supported by a Grant-in-Aid from the Ministry of Education, Culture, Sports, Science, and Technology of Japan (23590967), a grant from the Japanese Society of Gastroenterology, a grant from the Ministry of Health, Labor, and Welfare, and a grant from the National Cancer Center Research and Development Fund (23-B-5) of Japan. X.W.W. is supported by the Intramural Research Program of the Center for Cancer Research, U.S. National Cancer Institute.

epithelial cell adhesion molecule (EpCAM) and alpha-fetoprotein (AFP), which correlate with distinct gene-expression signatures and prognosis.[8,9] $EpCAM^+$ HCC cells isolated from primary HCC and cell lines show CSC features, including tumorigenicity, invasiveness, and resistance to fluorouracil (5-FU).[10] Similarly, other groups have shown that $CD133^+$, $CD90^+$, and $CD13^+$ HCC cells are also CSCs, and that EpCAM, CD90, and CD133 are the only markers confirmed to enrich CSCs from primary HCCs thus far.[3-5,10]

Although $EpCAM^+$, $CD90^+$, and $CD133^+$ cells show CSC features, such as high tumorigenicity, an invasive nature, and resistance to chemo- and radiation therapy, it remains unclear whether these cells represent an identical HCC population and whether they share similar or distinct characteristics. In this study, we used fluorescent-activated cell sorting (FACS), microarray, and immunohistochemistry (IHC) techniques to investigate the expression patterns of the representative liver CSC markers CD133, CD90, and EpCAM in a total of 340 HCC cases and 7 cases of mesenchymal liver tumors. We further explored gene- and protein-expression patterns as well as tumorigenic capacity of sorted cells isolated from 15 primary HCCs and 7 liver cancer cell lines in an attempt to identify the molecular portraits of each cell type.

Materials and Methods

Clinical Specimens. HCC samples were obtained with informed consent from patients who had undergone radical resection at the Liver Center in Kanazawa University Hospital (Kanazawa, Japan), and tissue acquisition procedures were approved by the ethics committee of Kanazawa University. A total of 102 formalin-fixed and paraffin-embedded HCC samples, obtained from 2001 to 2007, were used for IHC analyses. Fifteen fresh HCC samples were obtained between 2008 and 2012 from surgically resected specimens and an autopsy specimen and were used immediately to prepare single-cell suspensions and xenotransplantation (Table 1). Seven hepatic stromal tumors (three cavernous hemangioma, two hemangioendothelioma, and two angiomyolipoma) were formalin fixed and paraffin embedded and used for IHC analyses.

Table 1. Clinicopathological Characteristics of HCC Cases Used for Xenotransplantation

ID	Age/ Sex	Etiology	Tumor Size (cm)	Histological Grade	AFP (ng/mL)	DCP (IU/mL)
P1	77/M	Alcohol	12.0	Moderate	198	322
P2	61/F	NBNC	11.0	Moderate	12	3,291
P3	66/M	NBNC	2.2	Moderate	13	45
P4	65/M	HCV	4.2	Poor	13,700	25,977
P5	52/M	HBV	6.0	Moderate	29,830	1,177
P6	60/M	HCV	2.7	Poor	249	185
P7	79/F	HBV	4.0	Poor	46,410	384
P8	77/F	NBNC	5.5	Moderate	17,590	562
P9	71/M	Alcohol	7.0	Poor	3,814	607
P10	51/M	HBV	2.2	Well	<10	21
P11	71/M	Alcohol	2.1	Well	<10	11
P12	60/M	HBV	10.8	Poor	323	2,359
P13	66/M	HCV	2.8	Moderate	11	29
P14	71/M	HCV	7.2	Moderate	235,700	375,080
P15	75/M	HBV	5.5	Poor	<10	97

Abbreviation: DCP, des-gamma-carboxy prothrombin.

Additional details of experimental procedures are available in the Supporting Information.

Results

EpCAM, CD133, and CD90 Expression in HCC. We first evaluated the frequencies of three representative CSC markers ($EpCAM^+$, $CD90^+$, and $CD133^+$ cells) in 12 fresh primary HCC cases surgically resected by FACS (representative data shown in Fig. 1A). Clinicopathological characteristics of primary HCC cases are shown in Table 1. We noted that frequency of $EpCAM^+$, $CD90^+$, and $CD133^+$ cells varied between individuals. Abundant $CD90^+$ (7.0%), but almost no $EpCAM^+$, cells (0.06%, comparable to the isotype control) were detected in P2, whereas few $CD90^+$ (0.6%), but abundant $EpCAM^+$, cells (17.5%) were detected in P4. Very small populations of $EpCAM^+$ (0.09%), $CD90^+$ (0.04%), and $CD133^+$ cells (0.05%) were found in P12, but they were almost nonexistent in P8, except for $CD90^+$ cells (0.08%) (Fig. 1A). We further evaluated the expression of EpCAM, CD90, and CD133 in xenografts obtained from surgically resected samples (P13 and P15) and an autopsy sample (P14). As a whole, compared to the isotype control, 7 of 15 HCCs contained definite $EpCAM^+$ cells (46.7%), whereas only 3 HCCs

Address reprint requests to: Taro Yamashita, M.D., Ph.D., Department of General Medicine, Kanazawa University Hospital, 13-1 Takara-Machi, Kanazawa, Ishikawa 920-8641, Japan. E-mail: taroy@m-kanazawa.jp; fax: +81-76-234-4250.

View this article online at wileyonlinelibrary.com.
DOI 10.1002/hep.26168
Potential conflict of interest: Nothing to report.
Additional Supporting Information may be found in the online version of this article.

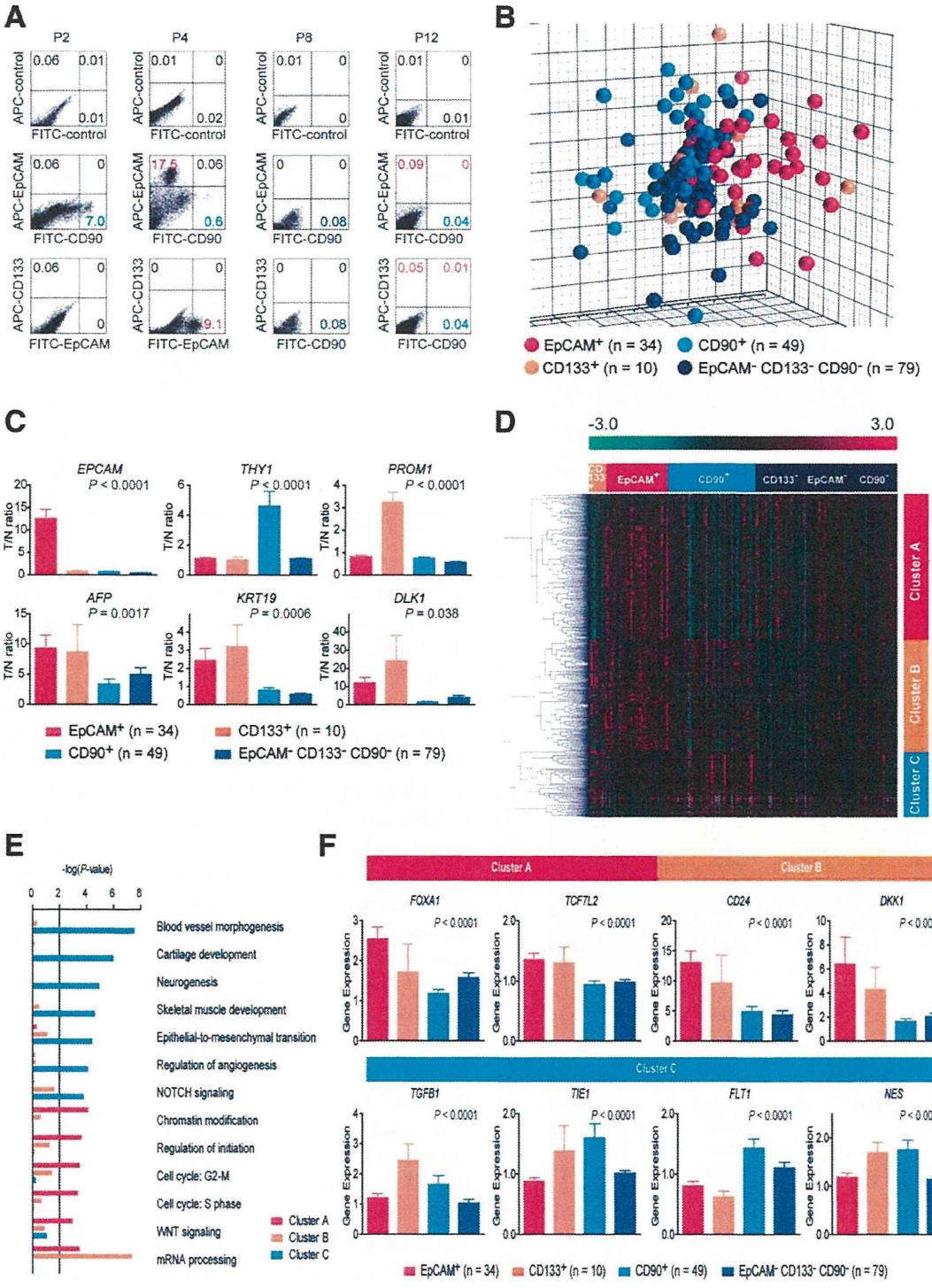

Fig. 1. Gene-expression profiles of CSC marker-positive HCCs. (A) FACS analysis of primary HCCs stained with fluorescent-labeled Abs against EpCAM, CD90, or CD133. (B) Multidimensional scaling analysis of 172 HCC cases characterized by the expression patterns of EpCAM, CD133, and CD90. Red, $EpCAM^{+}$ $CD90^{-}$ $CD133^{-}$ (n = 34); orange, $EpCAM^{-}$ $CD90^{-}$ $CD133^{+}$ (n = 10); light blue, $EpCAM^{-}$ $CD90^{+}$ $CD133^{-}$ (n = 49); blue, $EpCAM^{-}$ $CD90^{-}$ $CD133^{-}$ (n = 79). HCC specimens were clustered in specific groups with statistical significance ($P < 0.001$). (C) Expression patterns of well-known hepatic stem/progenitor markers in each HCC subtype, as analyzed by microarray. Red bar, $EpCAM^{+}$; orange bar, $CD133^{+}$; light blue bar, $CD90^{+}$; blue bar, $EpCAM^{-}$ $CD90^{-}$ $CD133^{-}$. (D) Hierarchical cluster analysis based on 1,561 EpCAM/CD90/CD133-coregulated genes in 172 HCC cases. Each cell in the matrix represents the expression level of a gene in an individual sample. Red and green cells depict high and low expression levels, respectively, as indicated by the scale bar. (E) Pathway analysis of EpCAM/CD90/CD133-coregulated genes. Canonical signaling pathways activated in cluster A (red bar), cluster B (orange bar), or cluster C (light blue bar) with statistical significance ($P < 0.01$) are shown. (F) Expression patterns of representative genes differentially expressed in EpCAM/CD90/CD133 HCC subtypes. Red bar, $EpCAM^{+}$; orange bar, $CD133^{+}$; light blue bar, $CD90^{+}$; blue bar, $EpCAM^{-}$ $CD133^{-}$ $CD90^{-}$.